Minireview

How the lipid-free structure of the N-terminal truncated human apoA-I converts to the lipid-bound form: new insights from NMR and X-ray structural comparison

Guangshun Wang*

Eppley Institute for Cancer Research, 986805 Nebraska Medical Center, University of Nebraska Medical Center, Omaha, NE 68198-6805, USA

Received 2 July 2002; revised 19 August 2002; accepted 23 August 2002

First published online 18 September 2002

Edited by Thomas L. James

Abstract The X-ray structure of the N-terminal truncated human apoA-I [Borhani et al., Proc. Natl. Acad. Sci. USA 94 (1997) 12291] and the NMR structure of intact human apoA-I [Okon et al., FEBS Lett. 517 (2002) 139] found similar repeating helices. The crystal structure is a twisted circular four-helix bundle, consisting of four molecules of apoA-I(44–243), where four copies of the lecithin:cholesterol acyltransferase (LCAT)-activating domains are located outside the ring structure, while the aromatic-rich strong lipid-binding domains are inside. This architecture suggests a lipid-binding mechanism that lipids directly enter the hole of the crystal structure. Indeed, four copies of Trp50 and Trp72 are exposed and oriented toward the center of the ring, initiating lipid binding. This is followed by the inside–out rotations of the terminal helices to make a belt with all the hydrophobic faces of the helices facing inward. Such lipid-binding induced rotations have an impact on the conformation of the lipid-free form. Indeed, the structure of residues 78–81 changes from helical (free) to disordered (bound) while the structure of residues 221–227 changes from extended to helical.

Key words: NMR; X-ray diffraction; High-density lipoprotein; Apolipoprotein A-I; Lipid binding; Aromatic residues

1. Human apoA-I is the major player in reverse cholesterol transport

It is well established that high-density lipoproteins (HDL) have a protective effect against atherosclerosis [1]. The protective effect of HDL is attributed to the reverse cholesterol transport pathway. This pathway includes cholesterol efflux from the tissue surface, esterification of free cholesterol by lecithin:cholesterol acyltransferase (LCAT), followed by delivering HDL back to the liver to be degraded [2]. The most abundant protein of HDL is apoA-I, which is the major player in the arena of reverse cholesterol transport. As a consequence, one of the approaches in antiatherogenic drug design is to mimic human apoA-I. It is, therefore, to our benefit to understand the structure and function of HDL, especially apoA-I.

The primary structure of 243-residue [3] apoA-I contains multiple 11- and 22-amino acid-residue repeating units [4]. These repeats were proposed to form amphipathic helices that are responsible for lipid binding [5,6]. Based on site-directed mutagenesis and synthetic peptide studies, the LCAT-activating domain of apoA-I has been mapped to residues 144–185 [7–10], whereas the N- and C-terminal regions are recognized as strong lipid-binding domains [11–13]. An N-terminal truncated apoA-I, namely, apoA-I(44–243), shares similar properties with intact apoA-I. Like intact apoA-I, apoA-I(44–243) shows no difference in binding lipids [14], and can form mature spherical HDL particles [15], supporting the concept that residues 1–43 constitute an independent domain. Further, significant progress has been made in the elucidation of the three-dimensional structure of human apoA-I [14,16–20]. The structure of apoA-I(44–243), elucidated by X-ray diffraction analysis in the absence of lipids, contains 10 helices [14], whereas the structure of intact apoA-I, determined in the lipid-mimetic micelles, contains 11 helices [19]. Based on the crystal structure, models for the discoidal [14,21] and spherical [14] HDL particles have both been proposed as belts wrapping around phospholipids.

The structural conversion from the lipid-free apoA-I to discoidal and spherical HDL particles is of fundamental significance in understanding the key process of reverse cholesterol transport. The molecular basis for such a structural conversion of apoA-I is not yet understood, although an open model has been proposed for the single-chain up-and-down helix-bundle structures by hinge rotation of a pair of helices by 180° for lipid binding [22–24]. This article proposes a novel mechanism for the structural conversion of apoA-I(44–243) from the free to lipid-bound form based on current structural data available for human apoA-I [14,17–20]. Since there is no high-resolution structure for the full-length lipid-free apoA-I, the possible mechanisms for its lipid binding are not discussed in this article.

2. The structures of human apoA-I(44–243) in the crystal and intact apoA-I in micelles are remarkably similar

Direct structural analysis of the heterogeneous lipoprotein particles by either high-resolution NMR spectroscopy or X-ray crystallography is still a challenging problem. The crys-

*Fax: (1)-402-559 4651.
E-mail address: gwang@unmc.edu (G. Wang).

0014-5793/02/$22.00 © 2002 Published by Elsevier Science B.V. on behalf of the Federation of European Biochemical Societies.
PII: S0014-5793(02)03354-9

tal structure of apoA-I(44–243) was solved in the absence of lipids [14]. On the other hand, NMR structures were elucidated in micelles (~50 Å) of dodecyl phosphocholine or sodium dodecyl sulfate, which mimic the lipid environment of the smallest HDL [17–20,25]. Similar helical structures were identified for the common region by X-ray crystallography for apoA-I(44–243) [14] (Fig. 1A) and by NMR spectroscopy for intact apoA-I [19] (Fig. 1B). Also, NMR analysis on the full-length apoA-I identified an additional helix, residues 8–32, at the N-terminal domain. The fact that 13 disordered residues separate the N-terminal helix (H0) from helix 1 (H1) supports the concept that the N-terminal domain of apoA-I, residues 1–43, functions as an independent domain. Human apoA-I structure is characterized by the modular nature as predicted from the amino acid sequence [5,6]. A typical structural module is the helix–hinge–helix motif [17]. This structure, originally found in apoA-I(142–187), is maintained in apoA-I(122–187), apoA-I(1–186) and intact apoA-I [17–19]. The structural units found in apoA-I(1–186) [18] recur in intact apoA-I [19]. The modular structure is also demonstrated by human apoC-I in a series of structural analyses from peptide fragments to intact protein [20,26]. A notable feature of this curved helix–hinge–helix structural motif is that hydrophobic residues occupy the same concave surface. Interestingly, a similar structure, including the same hydrophobic packing between Pro165 and Tyr166 in the hinge, was found in apoA-I(44–243) in the crystal [14]. In micelles, this structural motif interacts with lipids as confirmed by NMR using intermolecular NOESY experiments [17,25]. In the crystal, this structural motif interacts with three other apoA-I chains of the four-helix bundle. In addition to helices H6 and H7, the three-dimensional structures for helices H1–H3 (residues 50–101) are also strikingly similar in the crystal and micelles [20]. Hence, we conclude that the structural similarities of human apoA-I in the absence and presence of lipids are convincingly high, at least at the level of the secondary structure (Fig. 1).

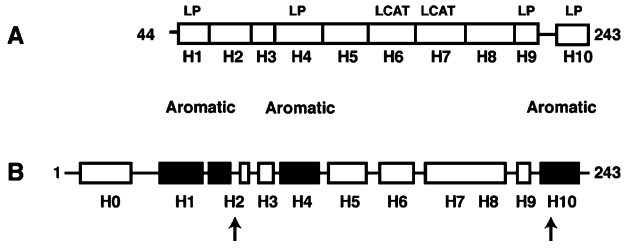

Fig. 1. NMR and X-ray structural comparison of apoA-I. Secondary structures of human apoA-I(44–243) (A) determined by X-ray crystallography in the lipid-free state [14] and intact human apoA-I (B) determined by NMR spectroscopy in SDS micelles [19]. Helices, represented by boxes, are labeled from H0 to H10 to be consistent with the convention in literature. Helical regions in apoA-I identified by X-ray (NMR) studies are H0, (8–32); H1, 50–65 (45–64); H2, 66–87 (67–77 and 82–86); H3, 88–98 (90–97); H4, 99–120 (100–118); H5, 121–142 (122–140); H6, 143–164 (146–162); H7, 165–186 (167–186); H8, 187–208 (187–205); H9, 209–219 (210–216); and H10, 228–243 (221–239). In micelles (B), H2 is split by a non-helical segment, residues 78–81, and residues 221–227 are helical (indicated by arrows). Strong lipid-binding helices are labeled with LP and the helices that activate LCAT are labeled with LCAT (reviewed in Ref. [13]). Aromatic-residue-rich regions, identified in this work, are represented by solid squares and labeled as aromatic (refer to Fig. 3A).

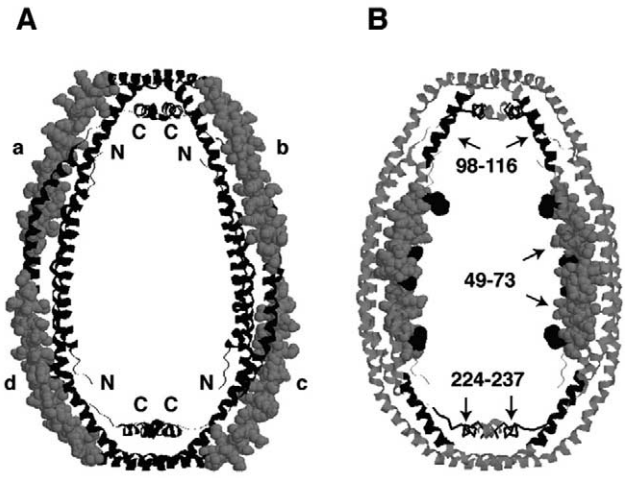

Fig. 2. Distinct locations of the functional domains of apoA-I in the circular views of the tetrameric crystal structure. A: Four copies of the LCAT-activating domain, residues 142–187, represented in the space-filling models (gray), occupy the outer circles of the distorted ring structure. The four apoA-I(44–243) chains (a–d) as well as the N-, and C-termini of the chain in the crystal structure are labeled. B: The strong lipid-binding domains rich in aromatic residues occupy the inner circles of the distorted ring structure. Residues 49–73, 98–116, and 224–237 are represented in the space-filling (gray, but the Trp residues in dark), ribbon (black), and backbone stick (black) models, respectively. For each of the aromatic-rich regions, only two copies are labeled by arrows due to symmetry. The PDB accession code for apoA-I(44–243) is 1av1 [14]. Figures were made using RasMol (http://www.umass.edu/microbio/rasmol).

This being said, some key structural differences in the two environments are worth pointing out. While a kink was observed at the proline residues in the crystal [14], NMR studies of apoA-I fragments and intact apoA-I in the micelles suggest two to five hinge residues between the repeating helices (Fig. 1B). These multiple 'hinges' in apoA-I are believed to be crucial for the plasticity of apoA-I, allowing it to adapt to HDL particles of a variety of different sizes and shapes [17–20]. Except for the end effect, other major structural differences lie in regions 78–81 and 221–227. In the crystal, residues 78–81 are helical while residues 221–227 are extended [14]. In contrast, residues 78–81 become disordered whereas residues 221–227 are helical in micelles [19].

3. The functional domains of apoA-I have distinct locations in the crystal structure

To see the location of the LCAT-activating domain in the crystal structure of apoA-I(44–243), helices H6 and H7 are represented in the space-filling model in a circular view of the crystal structure (Fig. 2A) [14]. Surprisingly, all four copies of the LCAT-activating domains are located outside of the tetrameric ring structure. In contrast, the strong lipid-binding domains, at the N- and C-termini of apoA-I(44–243), are located in the inner ring (Fig. 2A). Previous work on the LCAT-activating domain of apoA-I found that the amino acid sequence for that region is characterized by richness in arginines, lack in aromatic residues, and no hydrophobic pairs with (I, I+1) relationship in the sequence [17]. This is a weak lipid-binding region [13]. What will be the typical feature of those strong lipid-binding regions?

3.1. The strong lipid-binding regions are rich in aromatic residues

In Fig. 3A, a monomer of apoA-I(44–243) from the crystal is shown with aromatic residues, Trp, Phe and Tyr, represented in the space-filling model. Interestingly, these aromatic residues in the sequence are mainly clustered in three regions: residues 49–73 (4), 98–116 (4) and 224–237 (3), where the number of aromatic residues for each region is indicated in the parentheses. These aromatic-rich regions are predominantly located in the inner ring of the structure (Fig. 2B). On the other hand, lipid-binding studies identified residues 44–65, 100–121 and 210–241 as important lipid-binding regions [10–13,27]. Clearly, the three key lipid-binding regions in apoA-I correlate well with the three aromatic-rich regions found here (Fig. 1A), indicating that aromatic residues play an essential role in binding lipids. The NMR studies [20] indicate that helices H1 and H2 are essentially continual, supporting the current identification of the first aromatic-rich region as one of the important lipid-binding units. Earlier structural studies of apoE [28] and apoC-I [26] by NMR also pointed to the importance of aromatic residues in anchoring apolipoproteins to lipid micelles. These observations are consistent with the hydrophobicity scale analysis for membrane proteins that aromatic residues are especially favored at the interface [29]. A recent interesting study on an apoA-I-mimicking peptide showed that the property of the peptide alters with the addition of Phe residues to the hydrophobic face. Many biophysical and biochemical properties become optimal when four to five Phe residues are included [30]. This 'in vitro evolution' result is remarkably similar to the three to four aromatic residues found here in the aromatic-rich regions of apoA-I designed by nature for our best benefit.

3.2. Aromatic-aromatic interactions stabilize the lipid-free apoA-I(44–243) structure

Being prompted by the interesting finding above, we also looked into the distribution of aromatic residues in the entire tetrameric crystal structure of apoA-I(44–243). All Phe and Trp aromatic side chains are located in the inner ring of the structure, although the distribution of the Tyr residue varies (Fig. 3B). In the structure, these aromatic residues actually interact with each other. Two Tyr192 (chains b and c) pack with two Phe71 (chains a and d), forming a hydrophobic cluster (Fig. 3B). Starting from Tyr166, a train of aromatic residues, including Tyr100, Phe104, Trp108, Tyr115, Phe225, Phe229 and Tyr236, pack against one another. Two Tyr236 from chains a and b, or chains c and d, also stack together, consistent with an earlier report that the C-terminal domain of apoA-I plays a key role in protein aggregation [12]. Similarly, the aromatic-rich C-termini of apoE [31] and apoC-I [32], known to be important in lipid binding, are also essential for apolipoprotein aggregation. Hence, aromatic–aromatic in-

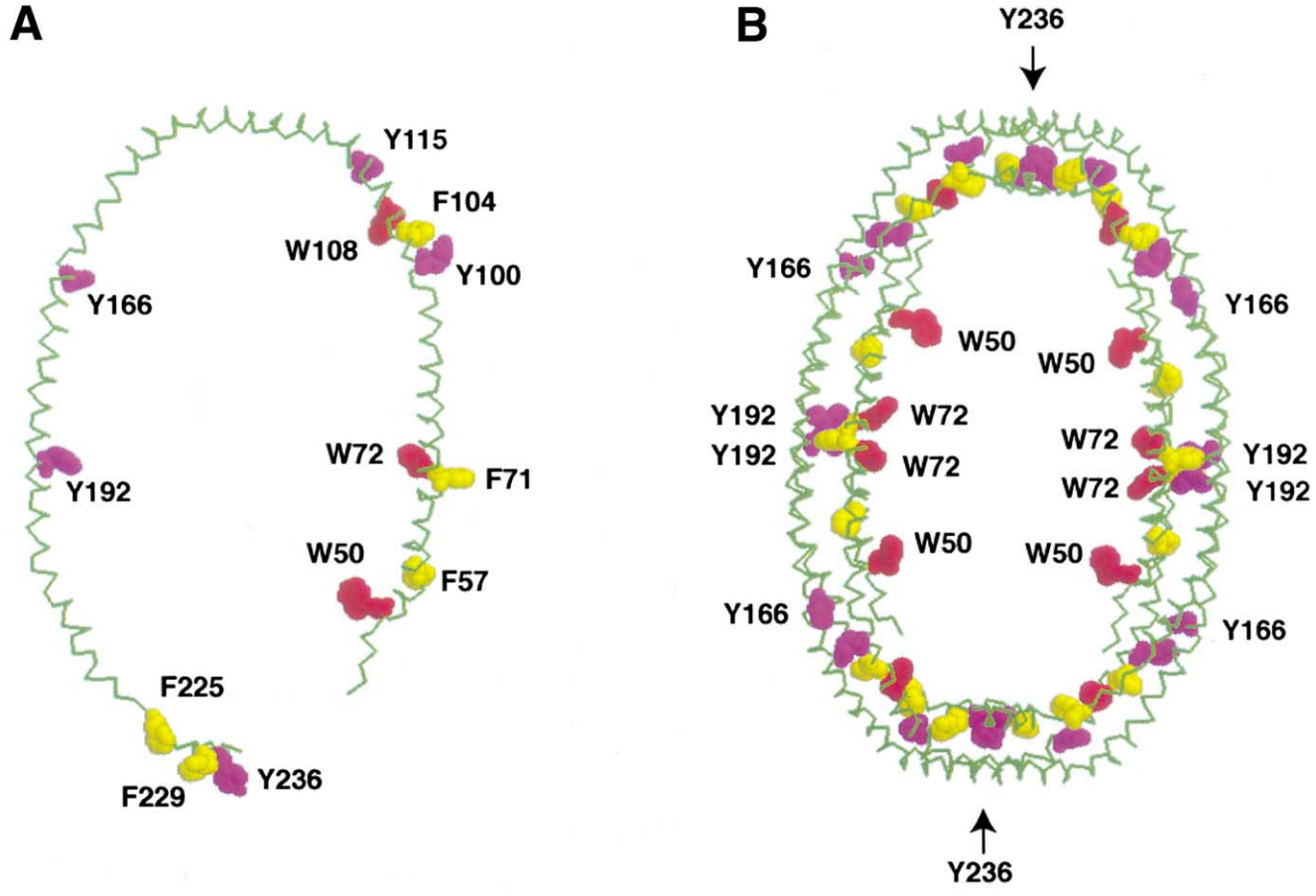

Fig. 3. Distribution of the aromatic residues of apoA-I(44–243) in the crystal structure of the (A) monomeric and (B) tetrameric forms. The aromatic residues are shown in the space-filling model. Color code: backbones in green, Trp in red, Phe in yellow, and Tyr in magenta. The arrows indicate one of the symmetry axes of the circular structure and also indicate the positions for the stacking Tyr236 at the C-terminus of apoA-I. Note that Trp50 and Trp72 are exposed on the inner curved surface of the structure (labeled with the single-letter amino acid code).

teractions [33] play a key role in apolipoprotein aggregation and in the stabilization of the helix-bundle structure of apoA-I(44–243). In strong contrast, eight Trp50 and Trp72, two from each chain, are exposed on the inner surface of the ring structure of apoA-I(44–243) and not involved in aromatic packing (Figs. 2B and 3B).

Before moving on further, it is pertinent to mention the resolution of the structure. The structure of lipid-free apoA-I(44–243) was originally solved at 4 Å and further refined to 3 Å using data collected at the synchrotron source. Further structural refinement did not make much difference. Because of the strong electron density of the aromatic rings and methionine residues, they have been useful in tracing the direction of the chains of apoA-I in the crystal [14]. Hence, the positions of aromatic side chains in the crystal are reasonably well determined with a confidence in $\chi 1$ angle greater than 75%. Also, the $\chi 2$ angles of Trp are pretty well defined because of the high electron density although the $\chi 2$ angles of Tyr and Phe are not as certain (D. Borhani, personal communication).

4. A model for the structural conversion of human apoA-I(44–243) from the free to lipid-bound form

The crystal structure of apoA-I(44–243) is a lipid-free form [14], while the NMR structure is the conformation of the monomeric apoA-I in micelles [19]. Assume that the micelle-associated conformation of apoA-I represents the lipid-bound form. This raises the question of how the helix-bundle structure of apoA-I(44–243) converts from the free to the lipid-bound state. A previous study on lipid binding of apoA-I(166–185), apoA-I(142–187) and apoA-I(122–187) revealed two mechanisms [17,25]. Lipid binding can be initiated either by electrostatic interactions between cationic side chains (mainly Arg) of these peptides and anionic lipids or by hydrophobic interactions between them, depending on the type of lipids. Since phospholipids and cholesterol are predominant in HDL with little anionic lipids, lipid binding of apoA-I(44–243) is more likely to be initiated by hydrophobic interactions.

The observation that strong lipid-binding domains are mainly located inside the tetrameric structure immediately suggests an attractive model for the structural conversion. In such a model, lipids are allowed to directly enter the hole of the pre-formed circular structure of apoA-I(44–243) and associate with the strong lipid-binding domains. A key question will be where such a lipid binding commences. This is puzzling since hydrophobic leucine and valine residues were noticed to be buried in the hydrophobic core of the helix bundle [14]. The analysis of the aromatic residues of apoA-I(44–243) in Section 3 turned out to be informative. While all the Phe and most of the Tyr residues are buried, it is exciting to note that the side chains of the four copies of Trp50 and Trp72 are actually exposed on the inner surface and oriented toward the pseudo-center of the elliptical ring structure of apoA-I(44–243) (Figs. 2B and 3B). In addition, close to Trp50, Leu44 and Leu47 are partially exposed (not shown). These exposed tryptophan regions are proposed to initiate lipid binding of the truncated apoA-I. Lipid anchoring by these exposed side chains can subsequently induce the structural re-arrangement of the protein to expose the buried hydrophobic surfaces for additional lipid binding. Because similar amphipathic helical structures have been observed in the lipid-free apoA-I(44–243) and lipid-bound intact apoA-I (Fig. 1), the structural conversion to the lipid-bound state may be achieved by simple terminal helix rotations around the long helix axis. The inside–out rotations for both C- and N-terminal strong lipid-binding helices are necessary to bring the hydrophobic surfaces of all the amphipathic helices into the same face to facilitate the belt to wrap around the lipid matrix as proposed in the belt model [14,21]. It is inevitable that such rotations will cause an increase or decrease in helical turns in apoA-I(44–243) before and after lipid binding. Indeed, there are structural differences between the lipid-free apoA-I(44–243) and lipid-bound apoA-I [14,19]. Upon lipid binding, residues 78–81 at the N-terminus change conformation from helical in the crystal to disordered in micelles. In contrast, residues 221–227 at the C-terminus change from extended in the crystal to helical in micelles (Fig. 1).

There are several lines of evidence supporting this model. First, tryptophan side chains exposed on the protein surface are hotspots for ligand binding [34]. These exposed Trp side chains are thus excellent candidates for initial lipid binding of apoA-I(44–243). Second, the side chains of tryptophans are always well defined in the micelle-bound structures of apolipoproteins and their segments [26,28], indicating the key role of these rigid aromatic rings in anchoring lipids. Indeed, the side-chain orientations of tryptophan in those apolipoprotein structures determined in micelles are consistent with an earlier finding of Landolt-Marticorena et al. [36] who showed that tryptophan is almost always found at the membrane–water interface, with the hydrophobic six-membered ring oriented toward the hydrophobic face and polarizable imino group intruding into the hydrophilic face. The locations of the three aromatic-rich regions of apoA-I in the strong lipid-binding domains are consistent with their role in binding lipids. The aromatic-rich N- and C-terminal regions have been implicated in the initial rapid lipid binding of apoA-I [10–12,16]. Third and more importantly, both in vitro and in vivo experiments [15] showed that further deletion of helix H1 from apoA-I(44–243) blocks the formation of spherical HDL particles [13,15]. In contrast, both intact apoA-I and apoA-I(44–243) yielded matured spherical HDL particles. Since the exposed Leu44, Leu47 and Trp50 residues belong to helix H1, this failure in structural conversion further reinforces the importance of these residues in initiating lipid binding and subsequent maturation of HDL. The structural conversion model proposed here for the N-terminal truncated apoA-I can be tested by site-directed mutagenesis. Whether this model applies to intact lipid-free apoA-I [16,35] may also be tested similarly even in the absence of a high-resolution structure.

In summary, the aromatic residues in apoA-I(44–243) have been proposed to play a key role in stabilizing the helix-bundle structure in the lipid-free state, in initiating lipid binding, and in stabilizing the lipid-bound structures. The unique lipid-binding mechanism proposed here for apoA-I(44–243) provides additional insight into the belt model [14,21]. It may also be crucial for rapid cholesterol binding by apoA-I and, thus, sheds light on the process of reverse cholesterol transport.

Acknowledgements: The author thanks Angie Rizzino, Barry Gold and Ken Cowan at the Eppley Institute for critical reading of the manuscript and Kristi Berger and Paul Keifer for proof reading.

References

[1] Breslow, J.L. (1996) Science 272, 685–688.
[2] Fielding, C.J., Shore, V.G. and Fielding, P.E. (1972) Biochem. Biophys. Res. Commun. 46, 1493–1498.
[3] Brewer Jr., H.B., Fairwell, T., LaRue, A., Ronan, R., Houser, A. and Bronzert, T.J. (1978) Biochem. Biophys. Res. Commun. 80, 623–630.
[4] McLachlan, A.D. (1977) Nature 267, 465–466.
[5] Segrest, J.P., Jackson, R.L., Morrisett, J.D. and Gotto Jr., A.M. (1974) FEBS Lett. 38, 247–253.
[6] Segrest, J.P., Graber, D.W., Brouillette, C.G., Harvey, S.C. and Anantharamaiah, G.M. (1994) Adv. Protein Chem. 45, 303–369.
[7] Sparrow, J.T. and Gotto Jr., A.M. (1982) CRC Crit. Rev. Biochem. 13, 87–107.
[8] Minnich, A., Collet, X., Roghani, A., Cladaras, C., Hamilton, R.L., Feilding, C.J. and Zannis, V.I. (1992) J. Biol. Chem. 267, 16553–16560.
[9] Sorci-Thomas, M., Kearns, M.W. and Lee, J.P. (1993) J. Biol. Chem. 268, 21403–21409.
[10] Holvoet, P., Zhao, Z., Vanloo, B., Vos, R., Deridder, E., Dhoest, A., Taverrne, J., Brouwers, E., Demarsin, E., Engelborghs, Y., Rosseneu, M., Collen, D. and Brasseur, R. (1995) Biochemistry 34, 13334–13342.
[11] Palgunachari, M.N., Mishra, V.K., Lund-Katz, S., Phillips, M.C., Adeyeye, S.O., Alluri, S., Anantharamaiah, G.M. and Segrest, J.P. (1996) Arterioscler. Thromb. Vasc. Biol. 16, 329–338.
[12] Ji, Y. and Jonas, A. (1995) J. Biol. Chem. 270, 11290–11297.
[13] Frank, P.G. and Marcel, Y.L. (2000) J. Lipid Res. 41, 853–872.
[14] Borhani, D.W., Rogers, D.P., Engler, J.A. and Brouillette, C.G. (1997) Proc. Natl. Acad. Sci. USA 94, 12291–12296.
[15] Scott, B.R., McManus, D.C., Franklin, V., McKenzie, A.G., Neville, T., Sparks, D.L. and Marcel, Y.L. (2001) J. Biol. Chem. 276, 48716–48724.
[16] Brouillette, C.G., Anantharamaiah, G.M., Engler, J.A. and Borhani, D.W. (2001) Biochim. Biophys. Acta 1531, 4–46.
[17] Wang, G., Sparrow, J.T. and Cushley, R.J. (1997) Biochemistry 36, 13657–13666.
[18] Okon, M., Frank, P.G., Marcel, Y.L. and Cushley, R.J. (2001) FEBS Lett. 487, 390–396.
[19] Okon, M., Frank, P.G., Marcel, Y.L. and Cushley, R.J. (2002) FEBS Lett. 517, 139–143.
[20] Cushley, R.J. and Okon, M. (2002) Annu. Rev. Biophys. Biomol. Struct. 31, 177–206.
[21] Segrest, J.P., Jones, M.K., Klon, A.E., Sheldahl, C.J., Hellinger, M., De Loof, H. and Harvey, S.C. (1999) J. Biol. Chem. 274, 31755–31758.
[22] Wilson, C., Wardell, M.R., Weisgraber, K.H., Mahkey, R.W. and Agard, D.A. (1991) Science 252, 1817–1822.
[23] Breiter, D.R., Kanost, M.R., Benning, M.M., Wesenberg, G., Law, J.H., Wells, M.A., Rayment, I. and Holden, H.M. (1991) Biochemistry 30, 603–608.
[24] Wang, J., Sykes, B.D. and Ryan, R.O. (2002) Proc. Natl. Acad. Sci. USA 99, 1188–1193.
[25] Wang, G., Treleaven, W.D. and Cushley, R.J. (1996) Biochim. Biophys. Acta 1301, 174–184.
[26] Rozek, A., Sparrow, J.T., Weisgraber, K.H. and Cushley, R.J. (1999) Biochemistry 38, 14475–14484.
[27] McManus, D.C., Scott, B.R., Frank, P.G., Franklin, V., Schultz, J.R. and Marcel, Y.L. (2000) J. Biol. Chem. 275, 5043–5051.
[28] Wang, G., Pierens, G.K., Treleaven, W.D., Sparrow, J.T. and Cushley, R.J. (1996) Biochemistry 35, 10358–10366.
[29] Wimley, W.C. and White, S.H. (1996) Nat. Struct. Biol. 3, 842–848.
[30] Datta, G., Chaddha, M., Hama, S., Navab, M., Fogelman, A.M., Garber, D.W., Mishra, V.K., Epand, R.M., Epand, R.F., Lund-Katz, S., Phillips, M.C., Segrest, J.P. and Anantharamaiah, G.M. (2001) J. Lipid Res. 42, 1096–1104.
[31] Westerlund, J.A. and Weisgraber, K.H. (1993) J. Biol. Chem. 268, 15745–15750.
[32] Gursky, O. (2001) Biochemistry 40, 12178–12185.
[33] Burley, S.K. and Petsko, G.A. (1985) Science 229, 23–28.
[34] Samanta, U. and Chakrabarti, P. (2001) Protein Eng. 14, 7–15.
[35] Narayanaswami, V. and Ryan, R.O. (2000) Biochim. Biophys. Acta 1483, 15–36.
[36] Landolt-Marticorena, C., Williams, K.A., Deber, C.M. and Reithmeier, R.A.F. (1993) J. Mol. Biol. 229, 602–608.